Directional sensing by cooperative chemoreceptor arrays modeled as Monod-Wyman-Changeux clusters

Jin Yang (□□)

Phys. Rev. E **87**, 032718 — Published 22 March 2013

DOI: 10.1103/PhysRevE.87.032718

Directional sensing by cooperative chemoreceptor arrays modeled as Monod-Wyman-Changeux clusters

Jin Yang (杨劲)*

Chinese Academy of Sciences – Max Plank Society Partner Institute and Key Laboratory for Computational Biology, Shanghai Institutes for Biological Sciences, Shanghai 200031, China and Department of Pathology and SpatioTemporal Modeling Center, University of New Mexico, Albuquerque, New Mexico 87131, USA

Most sensory cells use trans-membrane chemoreceptors to detect chemical signals in the environment. The biochemical properties and spatial organization of chemoreceptors play important roles in achieving and maintaining sensitivity and accuracy of chemical sensing. Here we investigate the effects of receptor cooperativity and adaptation on the physical limits for sensing chemical gradient. We study a single cell with aggregated chemoreceptor arrays on the cell surface and derive general formula to the limits for gradient sensing from the uncertainty of instantaneous receptor activity. In comparison to independent receptors, we find that cooperativity by non-adaptative receptors could significantly lower the sensing limits in a chemical concentration range determined by the biochemical properties of ligand-receptor binding and ligand-induced receptor activity. Cooperativity by adaptative receptors are beneficial to gradient sensing within a broad range of background concentrations. Our results also show that isotropic receptor aggregate layout on the cell surface represents an optimal configuration to gradient sensing.

PACS numbers: 87.16.dr, 87.17.Jj, 87.18.Tt

I. INTRODUCTION

Cellular sensory systems can detect and then respond to spatial and temporal changes of environmental signals. For example, bacteria sense chemical gradient by motion that translates spatial chemical concentration asymmetry into temporal asymmetry. Larger chemotactic eukaryotes are able to sense the spatial gradients of chemoattractants across the cell dimension. A primary task for a sensory cell is to respond to small chemical concentration changes or shallow chemical gradients with sufficient accuracy under stochastic noises. Berg and Purcell, in their classic study [1], showed that the fundamental physical limit of concentration sensing is set by the uncertainty of ligand arrivals to a sensory cell regardless of biochemical details in a sensing mechanism employed by the cell. This result was generalized by Bialek and Setayeshgar [2] using the fluctuation-dissipation theorem, and was also applicable to chemical gradient sensing [3].

Ligand detection by membrane-bound chemoreceptors is the first step in chemical sensing cascade in a vast majority of sensory systems of living cells. Uncertainty of ligand-receptor binding and stochastic dynamics of downstream cellular signaling may introduce additional noises. Reducing such noises can help a system to operate near the fundamental Berg-Purcell limit. However, the exact sensing limit under proper ligand-receptor interaction remains elusive. In particular, the effect of receptor cooperativity has recently been a focus of theoretical studies with different model assumptions predicting different outcomes [4–7]. Receptor cooperativity can sensitize the receptor response to small signal changes and in the meanwhile it also amplifies stochastic fluctuations in signal. Using a dynamic all-or-none global receptor coupling model in which receptor activity switches in a rate independent the strength of receptor cooperativity, Bialek and Setayeshgar [4] found that receptor cooperativity lowers the threshold of concentration sensing to help the cell to approach the Berg-Purcell limit. Hu *et al.* [5], by an Ising-type model, showed that receptor cooperativity reduces the instantaneous receptor noise within a shortened dynamic range of the background concentration. Most recently, Skoge *et al.* [7] studied receptor cooperativity by an Ising model with the Glauber dynamics (by which the rate of receptor activity switching is related to the extent of receptor coupling) and suggested that local receptor-receptor coupling could slow down receptor activity and thus could impair the signal-to-noise ratio due to critical slowing down in receptor response time.

Another crucial mechanism found in many cellular sensory systems is adaptation, which maintains sensitivity of systems to varying levels of environmental signals. It is well known that adaptation tunes kinetics of chemoreceptors at the molecular level. For the example of the better understood *E. coli*, the activity of receptors are modulated by multisite receptor methylation and demethylation. However, the effect of receptor cooperativity on chemical sensing limit under the context of receptor adaptation is yet to be fully examined.

Here we develop a theoretical model to investigate the role of receptor cooperativity on the accuracy of chemical sensing in the absence or presence of receptor adaptation. We consider a sensory cell with a hierarchical organization of cell-surface chemoreceptors. Receptor cooperativity is described by the classic MWC model [8], which was originally developed to explain allosteric regulation

* jinyang2004@gmail.com

of multi-subunit proteins and has been widely used to model chemoreceptor coupling in bacteria [9–12]. We derive formula for the limits of gradient sensing based on the uncertainty of instantaneous receptor states at the equilibrium. Our results indicate that cooperativity by non-adaptative receptors reduces instantaneous noise of receptor states within a limited range of background concentrations determined by the biochemical parameters of receptor dynamics and ligand-receptor binding. In contrast, cooperativity by adaptative receptors improves the sensing accuracy across a wide dynamic range. We also show that the layout of receptor aggregates on the cell surface significantly affects the sensing limit with the isotropic layout being the optimal. Although the sensing limit is sensitive to the cell orientation under anisotropic aggregate layouts, the effect of receptor cooperativity is geometrically invariant.

II. THEORY

A. A two-dimensional cell model

We consider a model (Fig. 1) for a two-dimensional chemotactic cell subject to a chemoattractant gradient field $\mathcal{G}(\mathbf{x}; p, \phi)$ with a steepness p and a direction ϕ, which specifies chemical concentration at spatial coordinate $\mathbf{x}$. The steepness is defined in a polar coordinate system as: $p \equiv \frac{r_0}{c_0}\frac{dc}{dr}$, a normalized concentration change across a reference distance r_0 along the direction of the gradient. The cell has M receptor aggregates distributed at distinct locations on the cell surface. Cooperative receptors form clusters of size n and each aggregate m contains N_m such

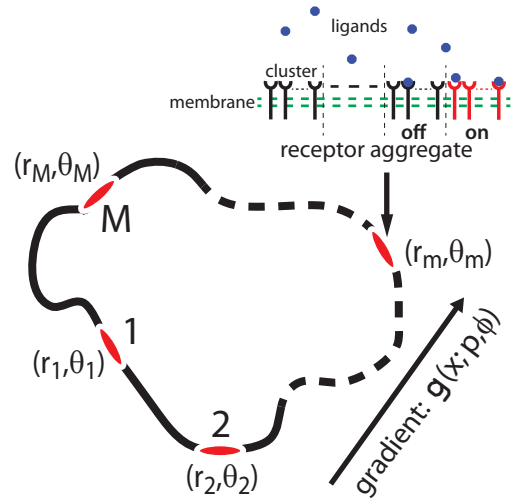

FIG. 1. (color online). A 2-D chemotactic cell with M chemoreceptor aggregates (patches labeled with polar coordinates (r_m, θ_m)) distributed on the cell surface (enclosed curve) under a gradient field $\mathcal{G}(\mathbf{x}; p, \phi)$ indicated by the arrow. Each receptor aggregate has $N_m, m = 1, ..., M$, cooperative receptor clusters of identical size n.

independent and non-interacting receptor clusters. The total number of receptor monomers in a cell is: $N_{\rm tot} = n\sum_{m=1}^{M} N_m$. This hierarchical organization of receptors on the cell membrane is general and can be parameterized to study a cell that has aggregated receptor arrays with $(n > 1)$ or without cooperativity $(n = 1)$ or has non-aggregated receptor monomers ($N_m = 1$ and $n = 1$).

In the absence of ligand, a receptor switches between active ("on") and inactive ("off") state with a free energy difference $\Delta E = E_{\rm off} - E_{\rm on}$ (in units of k_BT, where k_B is the Boltzmann constant and T is the absolute temperature). As in an MWC model, coupled receptors in a cluster switch in an all-or-none fashion between the "on" and "off" states. A ligand binds to a receptor of the "on" or "off" state with a dissociation constant $K_{\rm on}$ or $K_{\rm off}$, respectively. Ligand binding shifts the free energy difference between the two receptor states and such change can be sensed by a cell to measure the ligand concentration. At the equilibrium, a receptor cluster m at the "on" or "off" state bound to r ligands has the free energy of $nE_{\rm on} - \ln\left(\frac{[L]_m}{K_{\rm on}}\right)^r$ or $nE_{\rm off} - \ln\left(\frac{[L]_m}{K_{\rm off}}\right)^r$, $r = 0, ..., n$, respectively, with a multiplicity of $\binom{n}{r}$. Ligand concentration $[L]_m$ at the location of aggregate m is determined by the gradient field $\mathcal{G}(\mathbf{x}; p, \phi)$. From the Boltzmann distribution, the equilibrium probability for a receptor cluster in aggregate m to be active is given by [10, 11]:

$$P_m = \left[1 + \left(e^{-\Delta E}\frac{1 + c_m}{1 + \alpha c_m}\right)^n\right]^{-1}, \quad m = 1, ..., M \quad (1)$$

where $\alpha \equiv K_{\rm off}/K_{\rm on}$ and $c_m \equiv [L]_m/K_{\rm off}$.

At the equilibrium, an instantaneous configuration of receptor cluster states measures the chemical concentrations around the cell. Such configuration fluctuates in time due to stochasticity in ligand-receptor binding and in receptor state switching, which underlies the uncertainty in gradient sensing. Below we shall derive the best achievable limit for the sensing uncertainty.

The log likelihood for observing a specific configuration of cell-surface receptor states is:

$$\ln \mathcal{L}(p, \phi) = \ln \prod_{m=1}^{M} P_m^{k_m}(1 - P_m)^{N_m - k_m}, \quad (2)$$

where k_m is the number of active receptor clusters in aggregate m. An efficient unbiased estimator to parameters associated with the gradient field $\mathcal{G}(\mathbf{x}; p, \phi)$ has a variance limited by the optimal Cramer-Rao lower bound (CRLB) that can be determined from the likelihood function of Eq.(2). For convenience, define $(\psi_1, \psi_2) \equiv (p, \phi)$. The Fisher information matrix is given by [13]:

$$[\boldsymbol{I}]_{ij} \equiv \left\langle \frac{\partial \ln \mathcal{L}}{\partial \psi_i}\frac{\partial \ln \mathcal{L}}{\partial \psi_j} \right\rangle, \quad i, j = 1, 2, \quad (3)$$

where the expectation $\langle\cdot\rangle$ is taken with respect to the binomial distribution $f(k_m; P_m, N_m) = \binom{N_m}{k_m} P_m^{k_m}(1 -$

$P_m)^{N_m-k_m}$. We then have

$$[\boldsymbol{I}]_{ij} = \left\langle \sum_{m=1}^{M}\sum_{l=1}^{M} \frac{k_m - N_m P_m}{P_m(1-P_m)}\frac{\partial P_m}{\partial \psi_i}\frac{k_l - N_l P_l}{P_l(1-P_l)}\frac{\partial P_l}{\partial \psi_j} \right\rangle = \sum_{m=1}^{M}\sum_{l=1}^{M} \frac{\langle (k_m - N_m P_m)(k_l - N_l P_l)\rangle}{P_m(1-P_m)P_l(1-P_l)}\frac{\partial P_m}{\partial \psi_i}\frac{\partial P_l}{\partial \psi_j} \ .$$

Notice that the covariance $\langle (k_m - N_m P_m)(k_l - N_l P_l)\rangle = 0$ when $m \neq l$ due to independence of receptor aggregates. For $m = l$, the variance of k_m is $\left\langle (k_m - N_m P_m)^2 \right\rangle = N_m P_m(1-P_m)$. Therefore, the above Fisher information matrix becomes:

$$[\boldsymbol{I}]_{ij} = \sum_{m=1}^{M} \frac{N_m \left(\partial P_m/\partial c_m\right)^2}{P_m(1-P_m)}\frac{\partial c_m}{\partial \psi_i}\frac{\partial c_m}{\partial \psi_j} \ , \qquad (4)$$

where one can verify that

$$\frac{\partial P_m}{\partial c_m} = -nP_m(1-P_m)\frac{1-\alpha}{(1+c_m)(1+\alpha c_m)} \ . \qquad (5)$$

We define the coefficient

$$\omega_m \equiv \frac{N_m \left(\partial P_m/\partial c_m\right)^2}{P_m(1-P_m)} = \frac{N_m n^2 P_m(1-P_m)(1-\alpha)^2}{(1+c_m)^2(1+\alpha c_m)^2} \ , \qquad (6)$$

which is a function of local chemical concentration c_m, size of the receptor aggregate N_m, the strength of receptor coupling n and receptor affinities to the ligand $K_{\rm on}$ and $K_{\rm off}$. We first notice that for the single receptor aggregate m sensing its local chemical concentration c_m, the CRLB of the sensing variance is given as:

$$\sigma^2_{c_m} = \frac{1}{\omega_m} = \frac{(1+c_m)^2(1+\alpha c_m)^2}{N_m n^2 P_m(1-P_m)(1-\alpha)^2} \ . \qquad (7)$$

The noise-to-signal ratio is determined by $\sigma^2_{c_m}/c_m^2$.

For chemical gradient detection by all cell-surface receptor aggregates, the sensing limit to steepness p or direction ϕ is set by the CRLB's that are the diagonal entries of the inverted Fisher information matrix:

$$\sigma_p^2 = [\boldsymbol{I}^{-1}]_{11}, \quad \sigma_\phi^2 = [\boldsymbol{I}^{-1}]_{22} \ . \qquad (8)$$

To obtain analytical results, we assume that the cell resides in a linear gradient field. Across a typical cell size (*e.g.*, about 1 μm for *E. coli* or 10 μm for *Dictyostelium*), the linear gradient is a reasonable approximation. c_m at the polar coordinate (r_m, θ_m) is:

$$c_m = c_0[1 + \beta_m p\cos(\theta_m - \phi)] \ , \qquad (9)$$

where c_0 is the background concentration at the origin and the coefficient $\beta_m \equiv r_m/r_0$ is the distance from aggregate m to the origin normalized by the reference distance r_0. We have

$$\frac{\partial c_m}{\partial p} = c_0\beta_m\cos(\theta_m - \phi), \frac{\partial c_m}{\partial \phi} = c_0\beta_m p\sin(\theta_m - \phi) \ . \qquad (10)$$

One can now obtain the Fisher information matrix:

$$\boldsymbol{I} = c_0^2 \sum_{m=1}^{M} \omega_m \beta_m^2 \begin{bmatrix} \cos^2(\theta_m - \phi) & \dfrac{p\sin 2(\theta_m - \phi)}{2} \\ \dfrac{p\sin 2(\theta_m - \phi)}{2} & p^2\sin^2(\theta_m - \phi) \end{bmatrix} . \qquad (11)$$

In all cases, σ_p^2 and σ_ϕ^2 can be numerically computed, and it is possible to obtain their analytical solutions under special cell geometry and surface layout of receptor aggregates. Here we specialize to a circular cell of radius r and designate the origin as the cell center such that $\beta_m = \beta = r/r_0$, for all m. Under a shallow gradient across the cell length ($p\beta \ll 1$), we approximate $\omega_m \approx \omega_0$ for all receptor aggregates. ω_0 is calculated by Eq. (6) evaluated at concentration c_0, which can be considered as the average ligand concentration at the cell location (assigned to the cell center). For an equidistant layout of same-sized receptor aggregates over the cell surface (an isotropic distribution), we obtain the CRLB's for sensing p and ϕ [14]:

$$\sigma_p^2 = \frac{2(1+c_0)^2(1+\alpha c_0)^2}{N_{\rm tot}\beta^2\xi_n(1-\alpha)^2 c_0^2}, \quad \sigma_\phi^2 = \frac{\sigma_p^2}{p^2} \ . \qquad (12)$$

The factor $\xi_n \equiv nP_0(1-P_0)$ is related to receptor cooperativity n, where P_0 is calculated by Eq. (1) at c_0. The above limits in Eq.(12) have a few properties: (i) Both σ_p^2 and σ_ϕ^2 are independent of the number of receptor aggregates M and are insensitive to the gradient direction ϕ. (ii) Directional sensing improves (*i.e.*, σ_ϕ^2 decreases) as the steepness p increases. Fortuitously, σ_ϕ^2 is the noise-to-signal ratio of steepness sensing. (iii) The receptor system loses sensing capability when ligand binding does not differentiate the two receptor states ($\alpha \approx 1$). (iv) σ_p^2 is very sensitive to the cell size via the term $N_{\rm tot}\beta$, where $N_{\rm tot}$ may vary with the cell size by a certain relationship and therefore σ_p^2 could scale more strongly than the inverse of normalized cell radius β^2. Properties (iii) and (iv) also hold in the cases for anisotropic layouts of receptor aggregates.

The 2-dimensional model can be extended to a 3-dimensional one to approach a more geometrically realistic scenario. In the spherical coordinate system, a point has its spatial coordinate (r, ϑ, φ), where r is the radial length, ϑ and φ are the polar angle and the azimuthal angle. Assume a linear chemical gradient with a steepness p and a direction along the unit vector $\mathbf{g} \equiv [\cos\vartheta_g, \sin\vartheta_g\cos\varphi_g, \sin\vartheta_g\sin\varphi_g]$. The vector along the direction from origin O at the cell center to the location A_m of receptor aggregate m, OA_m, is $\mathbf{a}_m \equiv r_m[\cos\vartheta_m, \sin\vartheta_m\cos\varphi_m, \sin\vartheta_m\sin\varphi_m]$. Concentration c_m is given as:

$$c_m = c_0(1 + \frac{p}{r_0}\mathbf{a}_m \cdot \mathbf{g}) = c_0(1 + \beta_m p\cos\gamma_m) \ , \qquad (13)$$

where γ_m is the angle between $\mathbf{a}_m$ and $\mathbf{g}$. The dot product $\mathbf{a}_m \cdot \mathbf{g} = r_m\cos\gamma_m$ projects $\mathbf{a}_m$ onto the gradient

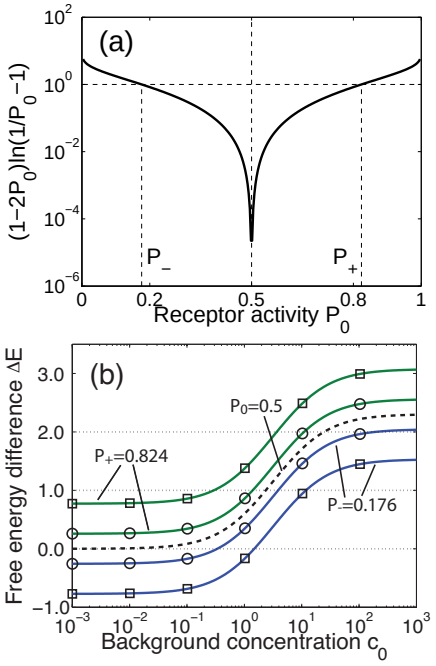

FIG. 2. (color online). (a). Function $(1-2P_0)\ln(1/P_0-1)$. Inequality Eq. (18) holds when $P_0 \in (P_-, P_+)$. (b) Solid curves show ΔE as a function of c_0 at $\alpha = 0.1$, $\Delta E = \ln(\frac{1+c_0}{1+\alpha c_0}) - \ln(1/P_+ - 1)/n$ (lower two curves) and $\Delta E = \ln(\frac{1+c_0}{1+\alpha c_0}) - \ln(1/P_- - 1)/n$ (upper two curves), for two cooperativity levels: $n = 2$ (□) and $n = 6$ (○). Upper and lower curves of same n enclose the regime that receptor cooperativity (up to n) helps to reduce the variance σ_p^2. The beneficial ranges of c_0 for three different ΔE values (2.0, 1.0, and 0) are marked by dotted lines (spanning boundaries specified by Eq. (20)). The dashed line indicates $P_0 = 1/2$. The results at $\alpha > 1$ (not shown) are clearly symmetric to those at $\alpha < 1$.

direction $\mathbf{g}$, with $\cos\gamma_m = \sin\vartheta_m \sin\vartheta_g \cos(\varphi_m - \varphi_g) + \cos\vartheta_m \cos\vartheta_g$. We have:

$$\frac{\partial c_m}{\partial p} = c_0\beta_m \cos\gamma_m \tag{14}$$

$$\frac{\partial c_m}{\partial \vartheta_g} = c_0\beta_m p(\sin\vartheta_m \cos\vartheta_g \cos(\varphi_m - \varphi_g) - \cos\vartheta_m \sin\vartheta_g) \tag{15}$$

$$\frac{\partial c_m}{\partial \varphi_g} = c_0\beta_m p \sin\vartheta_m \sin\vartheta_g \sin(\varphi_m - \varphi_g)\ . \tag{16}$$

The Fisher information matrix $\mathbf{I}$ can thus be constructed by Eq.(4), with the coefficient ω_m obtained by Eq.(6). Analytical formula like Eq.(12) can be obtained under special cell geometry and receptor aggregate layout on the cell surface. We will present our results for a 2D cell and expect the conclusions in general applicable to a 3D cell.

III. RESULTS

With a fixed number of receptors $N_{\rm tot}$, the effect of cooperativity on the gradient sensing limits described by Eq.(12) can be detected as the direction of change in ξ_n with regard to the receptor cluster size n:

$$\frac{\partial \xi_n}{\partial n} = P_0(1-P_0)\left[1 - n(1-2P_0)\left(\ln\frac{1+c_0}{1+\alpha c_0} - \Delta E\right)\right]. \tag{17}$$

Receptor cooperativity lowers the sensing limits when $\partial\xi_n/\partial n > 0$, which together with $P_0 = [1 + (e^{-\Delta E}\frac{1+c_0}{1+\alpha c_0})^n]^{-1}$ implies the constraint:

$$(1-2P_0)\ln\left(\frac{1}{P_0} - 1\right) < 1, \tag{18}$$

or equivalently,

$$P_- < P_0 < P_+\ , \tag{19}$$

where $P_- \approx 0.176$ and $P_+ = 1 - P_- \approx 0.824$ are the two solutions to: $(1-2P_0)\ln(1/P_0 - 1) = 1$ (see Fig.2(a) for illustration). The feasible range of ΔE, α and the background concentration c_0 is:

$$\frac{\ln(1/P_+ - 1)}{n} < \ln\left(\frac{1+c_0}{1+\alpha c_0}\right) - \Delta E < \frac{\ln(1/P_- - 1)}{n}\ , \tag{20}$$

within which receptor cluster of size up to n can improve the accuracy of chemical sensing. Fig. 2(b) shows that the beneficial region of free energy difference ΔE is confined in a banded area from around 0 at low ligand concentration to around $\ln(1/\alpha)$ at high ligand concentration. The bandwidth of ΔE, $\frac{2}{n}\ln(P_+/P_-)$, is limited by the cluster size n. A stronger cooperativity results in a narrower band. For each given ΔE, the beneficial range of background concentration c_0 is determined by Eq. (20) (see Fig.2(b) for illustration). The above derivation is under the assumption that the receptor system has a fixed total number of receptors $N_{\rm tot}$. The general conclusion also applies to a system that has fixed numbers of receptor clusters N_m in receptor aggregates [15].

In the following, we analyze the influence of receptor cooperativity on the chemical sensing limit under the context of receptors with or without adaptation.

A. Non-adaptative receptors

Without receptor adaptation, equilibrium receptor activity changes with the ligand concentration c_0 according to Eq. (1), where free energy difference ΔE and binding affinities $K_{\rm on}$ and $K_{\rm off}$ are unmodulated by receptor activity. Fig. 3 shows that in any case σ_p^2 assumes a valley-shaped relationship with the background concentration c_0. σ_p^2 attains a minimum at $d\sigma_p^2/dc_0 = 0$, *i.e.*:

$$2\alpha c_0^2 + n(1-\alpha)(1-2P_0)c_0 - 2 = 0\ . \tag{21}$$

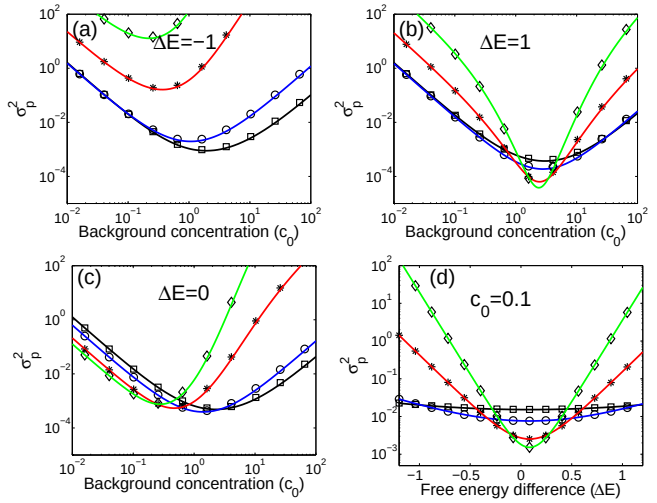

FIG. 3. (color online). σ_p^2 under varying background concentrations. Receptor aggregates have an equidistant layout on the cell surface. (a)-(d) were plotted with different ΔE (values indicated in plots) under different cluster size: $n = 1$ (non-cooperative), '□'; 2 (receptor dimer), '○'; 6, '∗' (corresponding to "trimer-of-dimers" in bacteria); and 10, '◇' (corresponding to an estimate by Ref. [11]). σ_p^2 were calculated by Eq. (8) (markers) and by Eq. (12) (solid lines) with $N_{\rm tot} = 80,000, M = 3, p = 0.1, \phi = 0$, $\alpha = 0.1$ and $\beta = 1$. σ_ϕ^2 behaves similarly and is not shown.

At the regime $\Delta E < 0$, where an unliganded receptor is biased to the "off" state, increasing receptor cooperativity always reduces sensing accuracy [Fig. 3(a)] when ligand binding also favors the "off" state (*i.e.*, $\alpha < 1$). According to Fig. 2(b), $\Delta E = -1$ is out of the band for receptor cooperativity to reduce the noise at any background concentration c_0. Intuitively, in this case, receptor arrays have limited capacity (most receptors are already "off" even before the introduction of ligands) to respond to ligand binding by further switching off receptor activity.

At the regime $\Delta E > 0$, receptor cooperativity reduces σ_p^2 within a concentration range around the optimal c_0 [Fig. 3(b)]. Such advantage is confined in a narrowed dynamic range around intermediate background concentrations [the stronger the cooperativity, the shorter the range of improvement] instead of being effective at lower concentrations, a desirable region for chemotactic responses. The results shown in Fig. 3(b) approximate those by the Ising-type model of Hu *et al.* [5] in which a receptor maintains the "on" state in the absence of ligand and is only switched off by ligand binding. In fact, the model by Hu *et al.* [5] can be considered as a limiting case to our model, by requiring $e^{-\Delta E} \ll 1$ and $\alpha \ll 1$.

By contrast, receptor cooperativity improves sensing accuracy below the optimal c_0 near $\Delta E \approx 0$ [Fig. 3(c)]. Fig. 3(d) shows that at low background concentration ($c_0 = 0.1$) the system achieves optimal sensing accuracy at free energy difference $\Delta E \approx 0$ of any cooperativity level and receptor cooperativity further decreases σ_p^2 (an order of magnitude improvement at $n = 10$ over independent receptors). One can relate this result to *E. coli*, in which $c_0 = 0.1$ corresponds to a background concentration of of ligand MeAsp at 2 nM, a threshold level, with $K_{\rm off} = 20$ nM and cooperativity predicted about $n = 10$ as in Ref. [11].

B. Adaptative receptors

Near precise receptor adaptation has been found in bacteria such as *E. coli* [16]. A ligand concentration change triggers a transient response in receptor activity followed by a slower decay back to the steady state about the prestimulus level. In other words, adaptation desensitizes the steady-state receptor activity to ligand concentration change, allowing the cell to be responsive to environmental signals within a wide dynamic range. Here we show that adaptation also conditions the receptor system to allow cooperativity to improve signal-to-noise ratio in chemical sensing under a wide range of background concentrations.

We assume that the adaptation machinery only adjusts the free energy difference ΔE and the receptor system is adapted to its chemical environment before an onset of change in ligand concentration. For the example of *E. coli*, receptor activity-controlled receptor methylation and demethylation act as a feedback mechanism that adjusts the free energy gap ΔE. Equilibrium receptor activity is tuned by adaptation into a constant, P_a, independent of the background concentration. At aggregate m, we have the adjusted free energy difference:

$$\Delta E_m = \ln \frac{1 + c_m}{1 + \alpha c_m} - \frac{1}{n} \ln \left(\frac{1}{P_a} - 1 \right) . \qquad (22)$$

Concentration changes around c_m induces transient receptor activity P_m away from P_a, which is evaluated by Eq.(1) at the adjusted ΔE_m.

The optimal sensing achieves at the half-activation level $P_a^* = 1/2$ that maximizes ξ_n, where $\sigma_p^2 = 8(1 + c_0)^2(1 + \alpha c_0)^2/(N_{\rm tot} n \beta^2 (1 - \alpha)^2 c_0^2)$. σ_p^2 attains a minimum of $\sigma_{p,\rm min}^2 = 8(\alpha^{1/2} + 1)^4/(N_{\rm tot} n \beta^2 (1 - \alpha)^2)$ at the background concentration $c_0 = \alpha^{-1/2}$ according to Eq. (21) [*i.e.*, $[L]_0 = (K_{\rm on} K_{\rm off})^{1/2}$, the geometric mean of dissociation constants]. As an example, Fig.2(b) shows (dashed line) the adjusted ΔE to adapted receptor activity $P_a = 1/2$ as a function of ligand concentration. The adaptation tunes ΔE into the middle of the beneficial region band and allows the receptor cooperativity to improve sensing of small concentration changes.

The adaptation mechanism may also likely maintain a constant steady-state activity by adjusting ligand binding affinities $K_{\rm on}$ and $K_{\rm off}$, or adjusting all three thermodynamics parameters altogether [17]. How adaptation tunes these parameters simultaneously remains unclear even for the well-studied *E. coli* chemoreceptors. Nonetheless, as our model shows, as long as the cell

achieves an adaptation level (precise or imprecise) that satisfies $P_- < P_a < P_+$, receptor cooperativity is advantageous for sensing small changes in chemical concentration or gradient. It has been suggested a precise adaptation of $P_a \approx 1/3$ in *E. coli* [18] which falls within the range specified by Eq. (19), supporting the idea that receptor adaptation and cooperativity act in concert to improve chemical sensing.

C. Effects of anisotropy in the layout of receptor aggregates

The analytical formula for the sensing limits (Eq. (12)) do not apply to the scenario where receptor aggregates anisotropically locate on the cell surface. As we will show, such an anisotropy may cause substantial dependence of σ_p^2 and σ_ϕ^2 on the gradient direction ϕ, the number and locations of receptor aggregates. To quantify the layout anisotropy, We define a metric:

$$\mathcal{R}_e = \frac{\sum_{i=1}^{M} |\theta_{i+1} - \theta_i - 2\pi/M|}{4\pi(M-1)/M}, \tag{23}$$

which is a normalized mean angular dispersion between two immediately aggregates from the average angular distance, $2\pi/M$. Without loss of generality, the angles of receptor aggregates are labeled in an order such that $\theta_{i+1} \geq \theta_i$, for $i = 1, .., M$, with the periodic boundary condition: $\theta_{M+1} \equiv \theta_1 + 2\pi$ (see Fig.1). $\mathcal{R}_e$ ranges from 0 for the isotropic case to 1 when all receptor aggregates gather at a single location.

Each receptor aggregate acts as a local concentration sensor, and a pair of spatially separate aggregates project the gradient onto the direction connecting the two aggregates. Two independent projections can reconstruct the gradient. In our model, two effective receptor aggregates are needed in minimum because of the implicit assumption that one parameter of the linear gradient, the background concentration c_0, is known. This assumption is justified by considering that the cell has a memory for a recent history of its chemical environment.

A sensing singularity occurs when the cell has only one effective receptor aggregate because two aggregates locate too close to each other, or has two aggregates lying on the opposite side across the cell center such that only one independent projection of the chemical gradient can be detected. In these cases, the Fisher information matrix becomes degenerate and the cell fails to resolve either gradient steepness or the direction. For $M = 2$, σ_p^2 diverges at either end, $\mathcal{R}_e = 0$ or 1, where the system has a single independent sensor [Fig. 4(a)]. For $M = 3$ or $M = 4$, σ_p^2 diverges at $\mathcal{R}_e = 1$ and a singularity of the sensing limit may also happen at $\mathcal{R}_e = 1/2$ or $2/3$, respectively. Notice that, as the number of receptor aggregates M increases, the extent of singularity decreases because receptor aggregate layouts with the corresponding value of $\mathcal{R}_e$ become less likely to degenerate by chance.

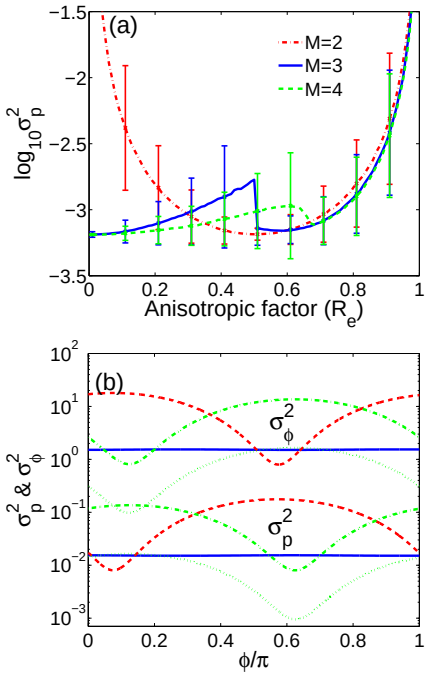

FIG. 4. (color online). Sensing limit under varying receptor aggregate layout and cell orientation (by non-adaptor receptors). (a) σ_p^2 vs. $\mathcal{R}_e$ ($n = 1$) at $M = 2$ (dashed dot), 3 (solid) and 4 (dashed). R_e was partitioned into 100 equispaced bins within the interval $(0, 1)$ and σ_p^2 was the geometric mean over 10,000 instances in each bin. Standard errors around the means are shown at several R_e values. (b) σ_p^2 (lower 4 curves) and σ_ϕ^2 (upper 4 curves), equidistance layout (solid) vs. two anisotropic layouts without receptor cooperativity: (i) $\mathcal{R}_e = 0.38$, $\theta_1 = 0.156\pi$, $\theta_2 = 1.08\pi$ and $\theta_3 = 1.99\pi$ (dashed) and (ii) $\mathcal{R}_e = 0.49$, $\theta_1 = 0.513\pi$, $\theta_2 = 1.66\pi$ and $\theta_3 = 1.68\pi$ (dashed dot), or with receptor coupling of size $n = 10$ for layout (ii) (dotted). Cell rotation is simulated by relatively varying ϕ from 0 to π. σ_p^2 and σ_ϕ^2 were calculated by Eq. (8) with parameter values $N_{\rm tot} = 80,000$, $M = 3$, $p = 0.1$, $c_0 = 0.1$, $\alpha = 0.1$, $\beta = 1$, and $\Delta E = 0$.

In general, one can verify that σ_p^2 may become singular at $\mathcal{R}_e = (M-2)/(M-1)$ and $\mathcal{R}_e = 1$ because some receptor aggregates locate so close to each other that they sense a same local ligand concentration or only detect a single gradient projection. Suppose among all adjacent aggregates along the cell circle there exist k angles that are equal to or greater than the average angle $2\pi/M$. Let Θ be the sum of these k angles. We then have:

$$\mathcal{R}_e = \frac{\Theta - 2\pi k/M}{2\pi(M-1)/M}, \tag{24}$$

changing from 0 to 1 as Θ ranges from $2\pi k/M$ to 2π. The aggregate layout can be classified into three cases when the value of k changes (see Fig. 5(a) for example layouts at $M = 3$). (i) When $k = 1$ and $\Theta = 2\pi$, $\mathcal{R}_e = 1$, the system has a single effective aggregate at one location ($\mathcal{R}_e = 1$), and therefore cannot resolve the gradient. The system is non-degenerate as long as $\Theta \neq 2\pi$. (ii) When

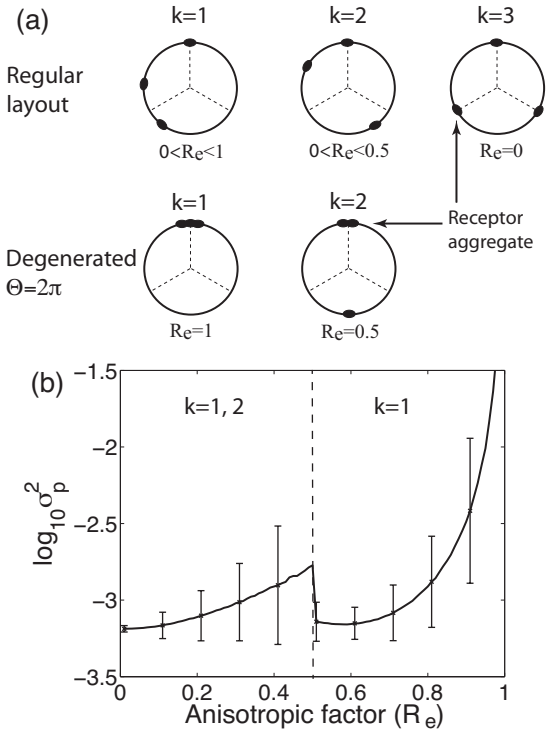

FIG. 5. (a) Sample layouts of receptor aggregates ($M = 3$). Note that $\mathcal{R}_e = 0.5$ corresponds to any scenario of the cell with two effective aggregates on cell surface and only the one shown with two aggregates on the opposite sides across the cell center is degenerate. Dashed lines inside the cell circle give a reference to an equiangular partition. (b) Correspondence between possible k values and $\mathcal{R}_e$ and their relationship with σ_p^2 (shown as the geometric mean with s.e.m.).

$k = 2$ and $\Theta = 2\pi$, $\mathcal{R}_e = (M-2)/(M-1)$, there exist two effective aggregates. When these two effective aggregates locate at two opposite sides on the circle across the cell center, the Fisher information matrix degenerates. The system is non-degenerate as long as $\Theta \neq 2\pi$. (iii) When $k \geq 3$, no degeneration appears. As an illustration for $M = 3$, Fig.5(b) shows that a singularity in σ_p^2 may happen at $\mathcal{R}_e = 0.5$ (corresponding to the last layout in Fig. 5(a)). However, the majority of layouts with $\mathcal{R}_e = 0.5$ are non-degenerate. For instance, all layouts with $k = 1$ and $\Theta = 4\pi/3$ has $\mathcal{R}_e = 0.5$ but none of them is degenerate.

Both σ_p^2 and σ_ϕ^2 are sensitive to the cell orientation under anisotropic aggregate layout [see Fig. 4(b) for a non-adaptive case]. The effect of receptor cooperativity is preserved under anisotropic receptor aggregate layouts because ξ_n is geometrically independent under a shallow gradient. By changing the cell orientation, improvement in estimating one parameter of p or ϕ is gained at the expense of the other. This result coincides with the study by Hu *et al.* [19] who showed that an elliptic cell cannot simultaneously improve limits σ_p^2 and σ_ϕ^2 by elongating the cell body. As an optimal configuration, the isotropic layout of receptor aggregates improves sensing both p and ϕ in most cases and is insensitive to cell orientation as indicated by Eq. (12) and as shown in Fig. 4(b). This result recapitulates the one derived by Berg and Purcell [1] who showed that uniformly distributed receptor patches on the membrane maximize independent ligand influx to the cell and thus sensitizes the concentration measurement. However, as shown by Fig. 4(b), proper cell orientation can improve estimation of one of the parameters (p or ϕ), which might be a desirable task if sensing one parameter is more critical than the other. For example, accurate directional sensing may be more important than steepness sensing in chemotaxis so that a cell can identify swimming direction more efficiently. The above results suggest that, for a cell with anisotropic layout of receptor aggregates, routine reorientation is required to improve sensing performance (e.g., tumbling of *E. coli*).

The minimal number and the optimal layout of receptor aggregates were obtained under the assumption that the background ligand concentration c_0 is known. One can also consider c_0 as an extra parameter to be estimated by the cell. In this case, merely by counting the number of parameters (p, ϕ and c_0) the cell needs in minimum three independent receptor aggregates as concentration sensors to reliably reconstruct the gradient. To compute the CRLB's, one must also calculate the derivative $\partial c_m/\partial c_0$ and obtain a 3-by-3 Fisher information matrix. The primary results about the sensing limits remain little changed. It is straightforward to verify that under isotropic receptor layout the variances of parameter estimates:

$$\sigma_p^2 = \frac{(2+\beta^2 p^2)(1+c_0)^2(1+\alpha c_0)^2}{N_{\rm tot}\beta^2\xi_n(1-\alpha)^2 c_0^2}, \tag{25}$$

$$\sigma_\phi^2 = \frac{\sigma_p^2}{(1+\beta^2 p^2/2)p^2}, \tag{26}$$

$$\sigma_{c_0}^2 = \frac{(1+c_0)^2(1+\alpha c_0)^2}{N_{\rm tot}\xi_n(1-\alpha)^2}\ . \tag{27}$$

Under a shallow gradient ($\beta p \ll 1$), σ_p^2 approaches the one derived in Eq. (12) while the variance of the directional sensing σ_ϕ^2 is unchanged. $\sigma_{c_0}^2$ is in a similarly form of Eq. (7) for detecting local concentration c_m by a single receptor aggregate.

IV. DISCUSSION AND CONCLUSION

It is well-known that adaptation brings the receptor activity back to pre-stimulus level, allowing the system to remain sensitive to chemical changes in the future. This mechanism enables the system to respond within a wide dynamic range of chemical concentration. Here we examine the role of adaptation in terms of chemical sensing accuracy, especially when presented with small signals or small changes in the signal, where stochastic noise may become overwhelming. Our study showed that receptor cooperativity reduces instantaneous noise only

within a limited background concentration range if the receptor aggregates do not undergo adaptation. By contrast, receptor adaptation, especially precise or near precise adaptation, maintains the receptor sensory system to operate within the parametric region where receptor cooperativity is beneficial. We note that this finding is consistent with the general result by fluctuation-dissipation theorem (FDT) [2] that relates sensitivity of a system to its instantaneous noise. The FDT states that the signaling gain of a system is proportional to the instantaneous noise, which implies that a mechanism that enhances sensitivity of the system will also help reduce its noise. It is well known that receptor cooperativity in chemotactic bacterial cells, such as the *e. coli*, sensitizes the cellular response to chemical signal as been observed in sharpened dose-responses, however, at the expense of a shortened dynamic range, which makes the receptor adaptation crucial to maintain the sensitivity [12, 17].

The sensing limits of Eq. (12) were derived from the uncertainty of a sampling of the gradient field by instantaneous receptor activities. As shown by Berg and Purcell [1], sensing accuracy can be further improved by a cell integrating independent receptor state configurations over time. The time interval between two independent measurements is determined by the correlation time τ_c that accounts for relaxation times of ligand diffusion, ligand-receptor binding [5] and receptor dynamics. The amount of time t available for averaging is limited by dynamics of the intracellular signaling circuit, which gives about $t/2\tau_c$ independent measurements [20]. Therefore, the temporal averaging reduces the instantaneous limit σ_p^2 to $\langle\sigma_p^2\rangle_t \approx 2\tau_c\sigma_p^2/t$ when $t \gg 2\tau_c$. Ligand concentration is encoded as receptor occupancy by the ligand-receptor binding and is then transduced into receptor activity by the MWC model. Stochastic dynamics at each stage of the signal transduction cascade contributes additional noise and thus increases the correlation time τ_c, which in consequence elevates the sensing uncertainty within the averaging time frame t.

The benefit of suppressing instantaneous receptor noise is biologically relevant if the averaging mechanism is separate from or weakly coupled to the one that determines the instantaneous noise itself (if at least below a certain degree of receptor coupling strength). Notably, the modeling study by Skoge *et al.* [7] recently showed that receptor cooperativity by local receptor coupling may significantly slow down receptor state switching to an extent such that the system cannot effectively relay ligand concentration changes in time. In other words, the correlation time τ_c is prolonged by receptor coupling and becomes comparable or greater than the averaging time t. In the model of Skoge *et al.*, the kinetics of receptor state switching was described by Glauber dynamics [21] originally developed for studying dynamics of the Ising model, in which the correlation time increases exponentially with the coupling strength between neighboring receptors. As a consequence, coupled receptors always performs inferior to independent receptors in signal-to-noise ratio for concentration sensing. This study suggested that receptor cooperativity observed in many chemotactic cells may not as previously assumed be selected for enhancing the chemical sensing accuracy. Further theoretical and experimental studies are required to elucidate in detail the interplay between receptor coupling and receptor dynamics and its effects on the accuracy of chemical sensing in specific biological systems. In particular, direct experimental evidence will shed light on how receptor coupling quantitatively modulates receptor dynamics in biological systems, which will help to develop more accurate models.

Another possible source of noise at the ligand-receptor interaction level is due to ligand rebinding when a dissociated ligand diffuses back again to bind onto the receptor aggregate before it escapes into the bulk medium. The extent of ligand rebinding and its effects on the accuracy of ligand sensing depend on the size and density of a receptor aggregate [22]. Theory [23] and simulation [24] showed that ligand rebinding does not change the equilibrium occupancy of individual receptors and therefore does not affect the sensing limits obtained from instantaneous measurement. However, significant ligand rebinding does introduce extra fluctuations by decreasing the effective rate constants for ligand association with and dissociation from the receptor, which increases the correlation time τ_c and thus reduces the number of independent measurements within a fixed averaging time.

Chemoreceptor cooperativity in bacteria was predicted by Ising models and MWC models used for analyzing dose response data in *E. coli* [9, 25]. Recent electron cryotomography evidence [26] has unveiled the hexagonal organization of *trimer-of-dimers* of chemoreceptors as a conserved architecture in a wide variety of bacteria. The spatial organization of eukaryotic chemoreceptors remains to be fully resolved, even though higher-order receptor arrays in chemotactic eukaryotes have also been observed [27], suggesting possible receptor coupling. Our model of the receptor organization on the cell surface is general and can be parameterized to study systems of coupling or non-coupling receptors with or without adaptation.

Berg and Purcell [1] showed that uniformly distributed receptor patches over the cell surface is optimal for reducing interactions between nearby receptors and therefore maximizes ligand intake by the cell, where ligands were considered spatially homogeneous in the environment. Here, we consider the detection of spatial asymmetry of ligand concentrations around the cell due to the chemical gradient. By examining the effect of geometric layout of receptor aggregates on the cell surface, we showed that anisotropic receptor aggregate distribution generates a trade-off between the sensing limit of gradient steepness p and that of the gradient direction ϕ (Fig.4). The isotropic layout represents an optimal configuration, in which the sensing accuracy is insensitive to cell orientation.

In summary, we study the effect of receptor coopera-

tivity and adaptation on the chemical sensing limit by evaluating the Cramer-Rao lower bounds from the instantaneous global state of receptor activity. Our results showed that receptor cooperativity with receptor adaptation increases gradient sensing accuracy (by lowering the CRLB) for small signal changes across a wide dynamic range of background concentration. This result is also applicable to concentration sensing at a single aggregate location (Eq. (7)). It remains largely unknown whether or how a chemotactic cell achieves its sensing limit. Receptor internalization [28] might improve chemical sensing by helping the cell membrane to function as an absorbing surface, an ideal device that operates at the fundamental Berg-Purcell limit. Maximum likelihood estimation (MLE) from ligand-receptor binding time series [29] or instantaneous receptor states [5, 19] was also suggested as a possible approach to the physical limit. The answer to how a cell mechanistically integrates information in time and space remains speculative and requires future investigations.

V. ACKNOWLEDGEMENT

We thank Qiang Chang, Byron Goldstein, Libo Huang and Zhen Wang for many helpful discussions. The work was supported by National Science Foundation of China through grant 30870477.

[1] H. C. Berg and E. M. Purcell, Biophys. J. **20**, 193 (1977).
[2] W. Bialek and S. Setayeshgar, Proc. Natl. Acad. Sci. USA **102**, 10040 (2005).
[3] R. G. Endres and N. S. Wingreen, Proc. Natl. Acad. Sci. USA **105**, 15749 (2008); Prog. Biophys. Mol. Biol. **100**, 33 (2009).
[4] W. Bialek and S. Setayeshgar, Phys. Rev. Lett. **100**, 258101 (2008).
[5] B. Hu, W. Chen, W. J. Rappel, and H. Levine, Phys. Rev. Lett. **105**, 48104 (2010).
[6] G. Aquino, D. Clausznitzer, S. Tollis, and R. G. Endres, Phys. Rev. E **83**, 021914 (2011).
[7] M. Skoge, Y. Meir, and N. S. Wingreen, Phys. Rev. Lett. **105**, 178101 (2011).
[8] J. Monod, J. Wyman, and J. P. Changeux, J. Mol. Biol. **12**, 88 (1965); J. P. Changeux, Annu. Rev. Biophys. **41** (2012).
[9] V. Sourjik and H. C. Berg, Nature **428**, 437 (2004).
[10] B. A. Mello and Y. Tu, Proc. Natl. Acad. Sci. USA **102**, 17354 (2005).
[11] J. E. Keymer, R. G. Endres, M. Skoge, Y. Meir, and N. S. Wingreen, Proc. Natl. Acad. Sci. USA **103**, 1786 (2006).
[12] M. L. Skoge, R. G. Endres, and N. S. Wingreen, Biophys. J. **90**, 4317 (2006).
[13] S. M. Kay, *Fundamentals of Statistical Signal Processing, Vol. I: Estimation Theory* (Prentice Hall, 1993).
[14] For an equidistant layout of receptor aggregates ($M \geq 3$), $\sum_{m=1}^{M} \cos^2(\theta_m - \phi) = \sum_{m=1}^{M} \sin^2(\theta_m - \phi) = M/2$ and $\sum_{m=1}^{M} \sin 2(\theta_m - \phi) = 0$.
[15] In this scenario, the factor related cooperativity is $\xi_n = n^2 P_0(1-P_0)$. $\partial \xi_n / \partial n > 0$ implies that $(1-2P_0)\ln(1/P_0 - 1) < 2$, or, $P_- < P_0 < P_+$, where $P_- \approx 0.083$ and $P_+ \approx 0.917$.
[16] H. C. Berg and D. A. Brown, Nature **239**, 500 (1972).
[17] B. A. Mello and Y. Tu, Biophys. J. **92**, 2329 (2007).
[18] D. Clausznitzer, O. Oleksiuk, L. Løvdok, V. Sourjik, and R. Endres, PLoS Comp. Biol. **6**, e1000784 (2010).
[19] B. Hu, W. Chen, W. J. Rappel, and H. Levine, Phys. Rev. E **83**, 021917 (2011).
[20] K. Wang, W. J. Rappel, R. Kerr, and H. Levine, Phys. Rev. E **75**, 061905 (2007).
[21] R. J. Glauber, J. Math. phys. **4**, 294 (1963).
[22] The effective rate constants under ligand rebinding are given as: $\tilde{k}_f = k_f/(1 + [R]k_f/k_+)$ and $\tilde{k}_r = k_r/(1 + [R]k_f/k_+)$, where $k_+ = 4Da$ is the diffusion limited on rate to a receptor aggregate of size a. $[R]k_f/k_+$ is the rebinding/escape ratio that characterizes the degree of influence by ligand rebinding.
[23] D. Shoup and A. Szabo, Biophys. J. **40**, 33 (1982); B. Goldstein and M. Dembo, **68**, 1222 (1995).
[24] S. S. Andrews, Phys. Biol. **2**, 111 (2005).
[25] V. Sourjik and H. Berg, Proc. Natl. Acad. Sci. USA **99**, 123 (2002).
[26] A. Briegel, D. Ortega, E. I. Tocheva, K. Wuichet, *et al.*, Proc. Natl. Acad. Sci. USA **106**, 17181 (2009); A. Briegel, M. Beeby, M. Thanbichler, G. J. Jensen, *et al.*, Mol. Microbiol. **82**, 748 (2011); A. Briegel, X. Li, A. M. Bilwes, K. T. Hughes, *et al.*, Proc. Natl. Acad. Sci. USA **109**, 3766 (2012); J. Liu, B. Hu, D. R. Morado, S. Jani, M. D. Manson, and W. Margolin, **109**, E1481 (2012).
[27] G. H. Wadhams and J. P. Armitage, Nat. Rev. Mol. Cell Biol. **5**, 1024 (2004).
[28] G. Aquino and R. G. Endres, Phys. Rev. E **81**, 21909 (2010).
[29] R. G. Endres and N. S. Wingreen, Phys. Rev. Lett. **103**, 158101 (2009); T. Mora and N. S. Wingreen, **104**, 248101 (2010).